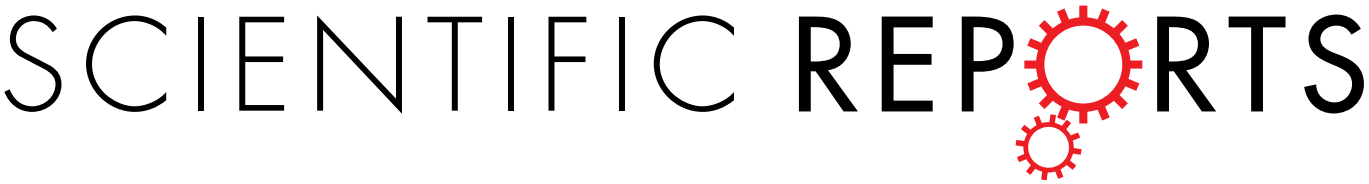

OPEN

Effect of adipose-derived mesenchymal stem cell transplantation on vascular calcification in rats with adenine-induced kidney disease

Received: 2 June 2017
Accepted: 11 October 2017
Published online: 25 October 2017

Shinya Yokote[1], Yuichi Katsuoka[2], Akifumi Yamada[3], Ichiro Ohkido[1] & Takashi Yokoo[1]

Previous studies have investigated the use of mesenchymal stem cells (MSCs) to treat damaged kidneys. However, the effect of adipose-derived MSCs (ASCs) on vascular calcification in chronic kidney disease (CKD) is still poorly understood. In the present study, we explored the potential of ASCs for the treatment of CKD and vascular calcification. CKD was induced in male Sprague-Dawley rats by feeding them a diet containing 0.75% adenine for 4 weeks. ASCs transplantation significantly reduced serum inorganic phosphorus (Pi) as compared to that in the control. The histopathology of the kidneys showed a greater dilation of tubular lumens and interstitial fibrosis in the control group. Calcium and Pi contents of the aorta in the ASCs transplantation group were lower than those in the control group. Von Kossa staining of the thoracic aorta media revealed that ASCs transplantation suppressed vascular calcification. Thus, this study revealed that autogenic ASCs transplantation inhibits kidney damage and suppresses the progression of vascular calcification in the CKD rat model, suggesting that autogenic ASCs transplantation is a novel approach for preventing the progression of CKD and vascular calcification.

Chronic kidney disease (CKD) is a major public health problem worldwide because end-stage renal disease (ESRD) is associated with cardiovascular morbidity and mortality[1,2]. Regardless of advances in supportive therapy for CKD, 2.6 million people received renal replacement therapy worldwide in 2010. Because of the increase in the number of patients with ESRD, the worldwide use of replacement therapy is projected to more than double by 2030[3]. Therefore, new modalities to prevent the progression of CKD and vascular calcification are desperately needed.

In the last few decades, advances in stem cell biology have led to the development of stem cell-based therapies, and many researchers have investigated the potential of stem cells for kidney regeneration[4–11]. We have succeeded in regenerating a functional kidney *de novo* using the kidney development program in rat embryos by applying human mesenchymal stromal cells (MSCs) at the niche of organogenesis[4,5]. Human MSCs are multipotent cells that can be isolated from several tissues and expanded *ex vivo* for clinical use[12,13]. They have also been shown to accelerate recovery and prevent acute or chronic renal failure in multiple disease models[14–19], thus providing novel strategies for kidney regeneration. MSCs have been reported to enhance angiogenesis[20,21], and conversely induce vascular remodelling[22] and calcification in a hyperlipidemic rat model[23]. Furthermore, MSCs alter osteoblast differentiation during metabolic acidosis and uremic conditions[24,25]. Thus, it is important to investigate the effect of MSCs transplantation on vascular calcification in patients with CKD. However, such effects have not been evaluated to date.

[1]Division of Nephrology and Hypertension, Department of Internal Medicine, The Jikei University School of Medicine, 3-25-8 Nishi-shimbashi, Minato-ku, Tokyo, 105-8461, Japan. [2]Department of Urology, St. Marianna University School of Medicine, 2-16-1, Sugao, Miyamae-ku, Kawasaki, Kanagawa, 216-8511, Japan. [3]Department of Pediatrics, The Jikei University School of Medicine, Tokyo, Japan. Correspondence and requests for materials should be addressed to T.Y. (email: tyokoo@jikei.ac.jp)

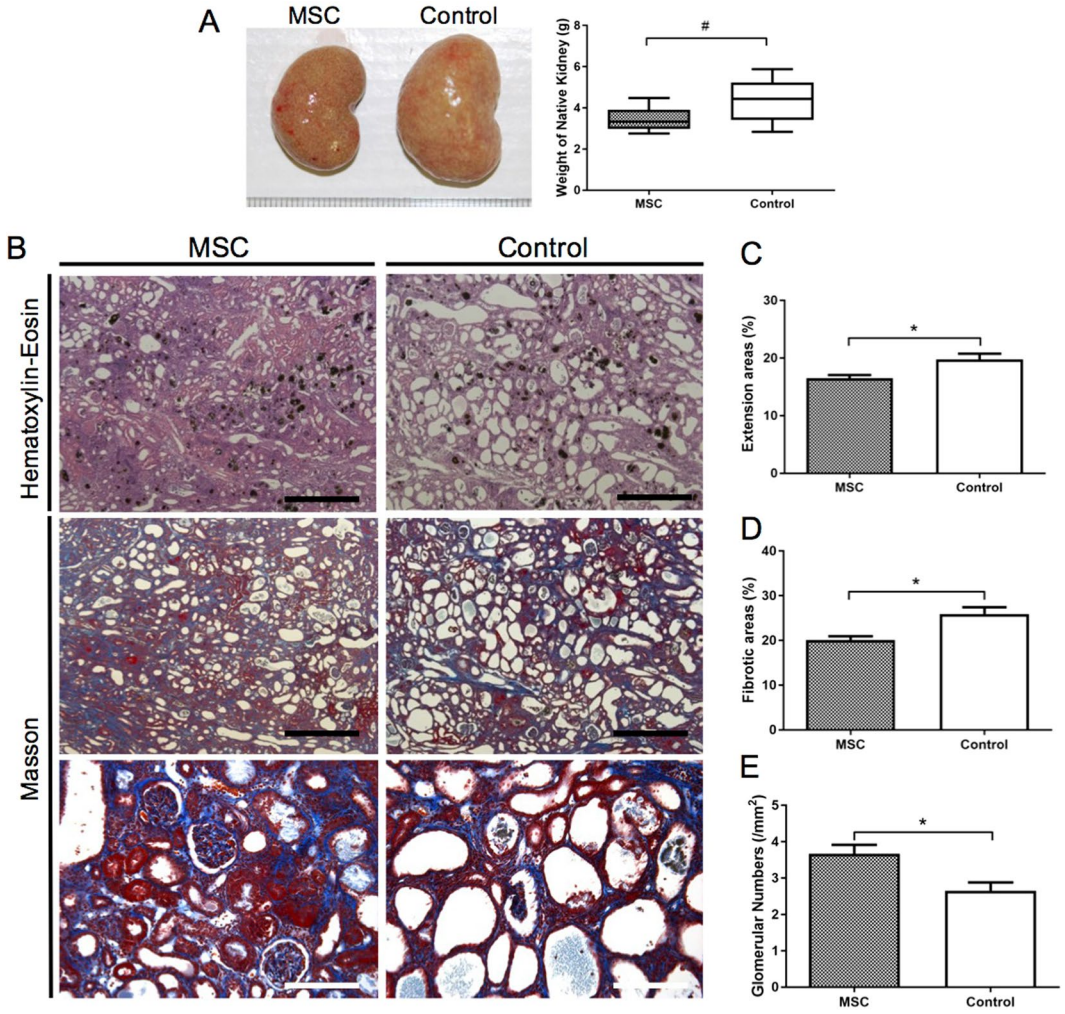

Figure 1. Histopathology of the kidneys in adenine-fed rats. (**A**) The average kidney weight in the control group was higher than that in the MSC group ($P < 0.005$). (**B**–**E**) Histopathological analysis of kidneys by haematoxylin–eosin staining and Masson-trichrome staining. Distention of tubular lumens ($P < 0.01$), interstitial fibrosis ($P < 0.005$), and reduction in glomerular numbers ($P < 0.005$) were observed in the control group as compared to those parameters in the MSC group. Data are expressed as the mean ± SEM. Black scale bars: 500 μm, white scale bars: 100 μm.

The adenine-induced kidney disease model is a well-established and widely used CKD model and is associated with vascular calcification[25–28], in which chronic tubulointerstitial nephritis is caused by the accumulation of 2,8-dihydroxyadenine crystals in the renal tubules and interstitium. Moreover, because arterial medial calcification develops in adenine-induced CKD rats with hyperphosphatemia, the adenine-induced model has been used as a model of uremic vascular calcification.

In the present study, we investigated the effects of transplanting autologous ASCs into rats with adenine-induced CKD on vascular calcification.

Results

MSCs isolation. MSCs were isolated from 9-week-old Sprague-Dawley (SD) rats. Characterization of MSCs cultured in standard culture medium showed a spindle-shaped morphology. Surface markers of MSCs were characterized by flow-cytometric analysis. MSCs were positive for CD90 (97.05 ± 1.25%) and CD29 (97.46 ± 0.25%), and negative for CD31 (0.72 ± 0.26%) and CD45 (1.16 ± 0.20%) (Supplementary Fig. S1A). MSCs had the capacity to differentiate into adipogenic, chondrogenic, and osteogenic lineages (Supplementary Fig. S1B–E).

MSCs transplantation reduces adenine-induced kidney injury. In the first experiment (Experiment 1 in the Materials and Methods), we aimed to assess the effects of MSCs transplantation on the pathology of CKD induced by 4 weeks of an adenine-supplemented diet in SD rats. The baseline characteristics of control and MSCs-administered rats before sacrifice are outlined in Supplementary Table 1. There were no differences between the control and MSC groups. After 4 weeks of the adenine-supplemented diet, the average kidney weight in the control group was higher than that in the MSC group (Fig. 1A). Histopathology of the kidney showed greater dilation of tubular lumens ($P < 0.01$), smaller glomerular numbers ($P < 0.01$), and higher interstitial

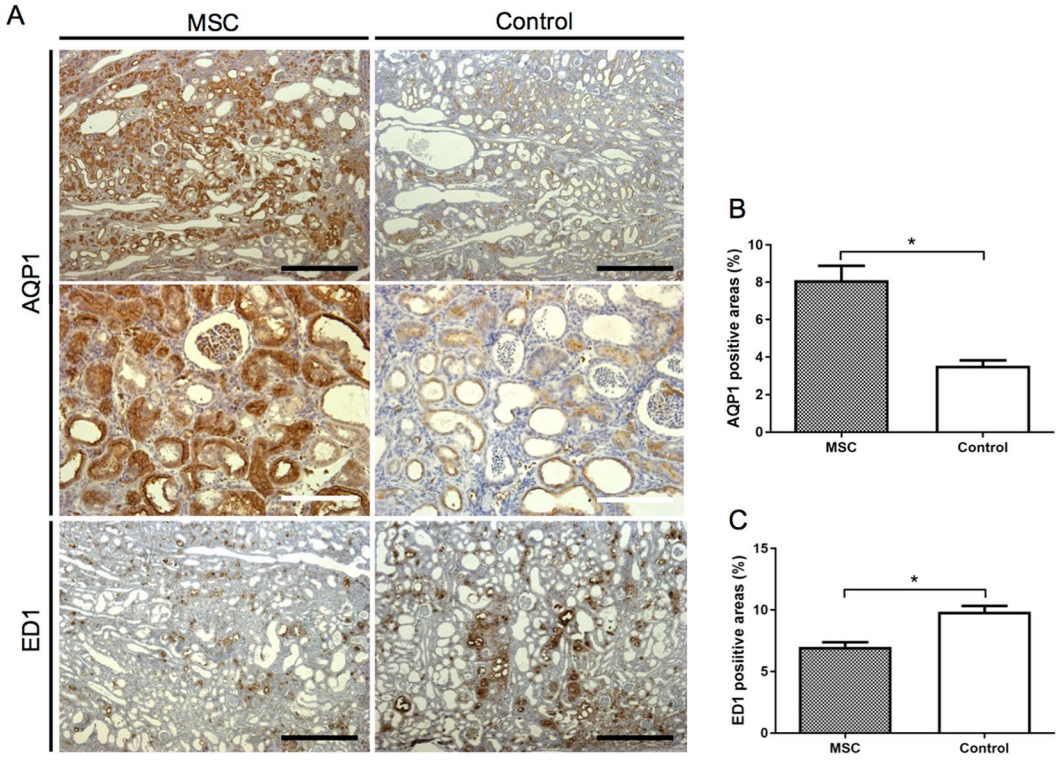

Figure 2. Immunohistopathology of kidneys from adenine-fed rats. (**A**) Immunohistopathological expression of AQP1 and ED1. (**B**) Mesenchymal stem cells (MSCs) transplantation significantly increased the AQP1-positive area ($P < 0.0001$) and (**C**) reduced the ED1-positive area ($P < 0.0005$) as compared to the those in control group. Data are expressed as the mean ± SEM. Black scale bars: 500 μm, white scale bars: 100 μm.

fibrosis ($P < 0.005$) in the control group than in the MSC group (Fig. 2B–E). Immunohistopathological analysis revealed that MSCs transplantation significantly increased AQP1-positive areas and reduced ED1-positive areas as compared to those with control treatment (Fig. 2).

The levels of blood urea nitrogen (BUN), creatinine (Cr), and inorganic phosphorus (Pi) increased over time with adenine feeding in rats of both groups (Fig. 3A–C). Although the levels of BUN and Cr in the MSC group on day 42 were lower than those in the control group (Fig. 3A, $P < 0.05$), the levels on day 56 did not significantly differ between both groups. However, the level of Pi in the MSC group on day 56 was lower than that in the control group (Fig. 3C, $P < 0.05$). Urinary parameters showed that MSCs transplantation significantly raised 24-hour creatinine clearance (24-h CCr) ($P < 0.05$), urinary Cr excretion ($P < 0.005$), and tubular reabsorption of phosphate (%TRP) ($P < 0.005$) as compared to those with control treatment (Fig. 4A–C). Furthermore, MSCs transplantation significantly decreased serum levels of fibroblast growth factor-23 (FGF23) and intact parathyroid hormone (PTH) levels as compared to those with control treatment (Fig. 3E,G). These results suggested that MSCs transplantation reduces adenine-induced kidney damage including interstitial fibrosis and tubular disorder due to interstitial nephritis, resulting in a reduction in serum Pi.

MSCs transplantation prevents the progression of vascular calcification. Histopathological von Kossa staining of the thoracic aorta media revealed vascular calcification in the control group, which was suppressed in the MSC group, after 4 weeks of adenine-supplemented diet (Fig. 5A). Calcification scores in the MSC group were significantly lower than those in the control group (Fig. 5D; $P < 0.05$). In the control group, calcium (Ca) and inorganic phosphorus (Pi) levels in the thoracic aorta were elevated; however, the increased Ca and Pi levels seen in the control group were significantly suppressed in the MSC group (Fig. 5B,C; $P < 0.0005$ and $P < 0.01$, respectively). Immunohistochemistry showed reduced expression of osteopontin (OP), Runx2, and fibronectin in the MSC group (Fig. 6A). The mRNA expression of OP (Fig. 6B; $P < 0.05$), Runx2 (Fig. 6C; $P < 0.05$), and fibronectin (Fig. 6D; $P < 0.05$) was also significantly suppressed in the MSC group as compared to that in control rats.

Injected MSCs are not detected in the damaged kidney and aorta. In Experiment 2, we used luciferase-expressing (Luc+) MSCs to assess the distribution of MSCs *in vivo*. Luc+ MSCs accumulated only in the lungs, likely as a result of being trapped in the pulmonary capillaries (Fig. 7A). The Luc signal disappeared within two days after transplantation. Luc+ MSCs did not home to damaged kidneys or the thoracic aorta via the lungs. Immunohistochemical staining confirmed that Luc+ MSCs did not migrate into the injured kidneys and thoracic aorta at the time of sacrifice (Fig. 7B). These results suggested that the therapeutic effect of MSCs on

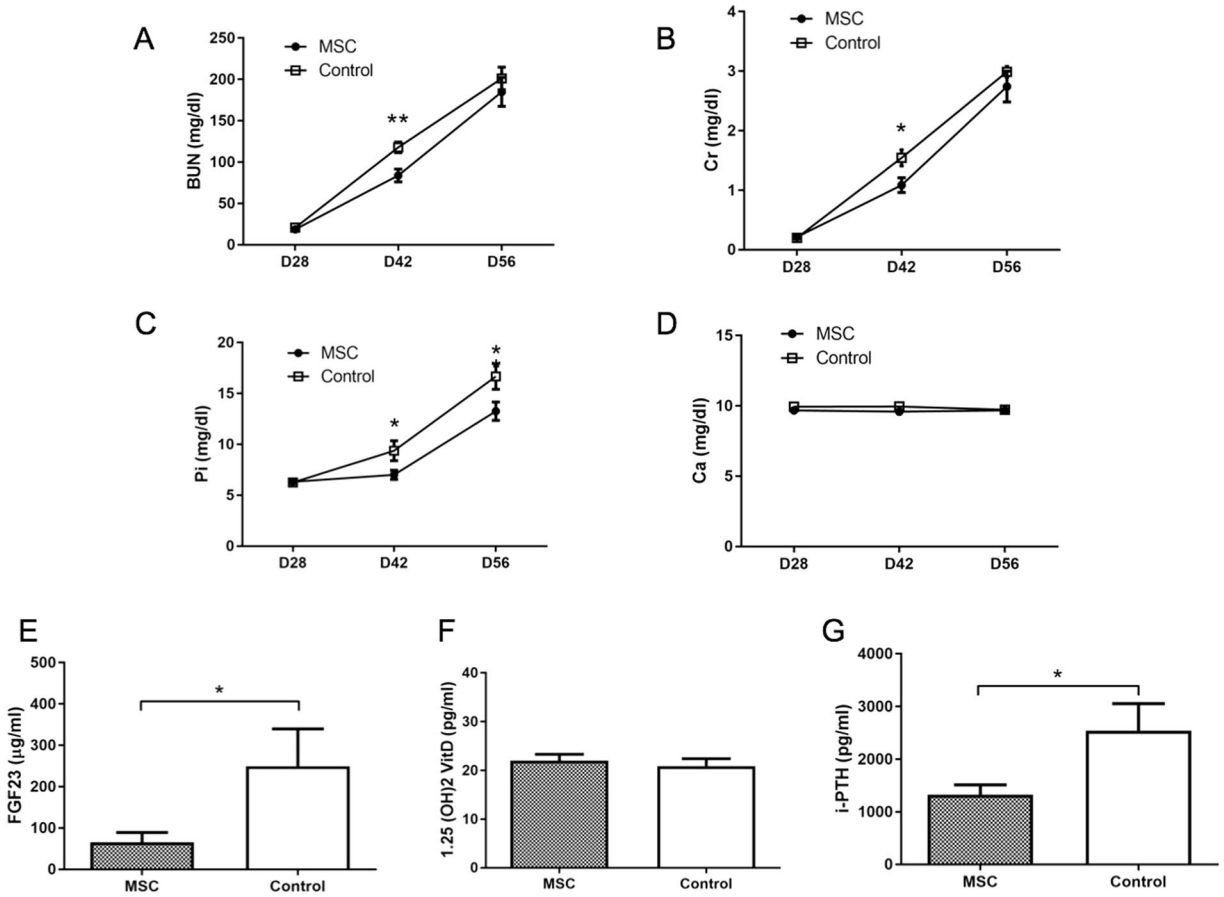

Figure 3. Serum parameters in adenine-fed rats. (**A**–**G**) Serum levels of blood urea nitrogen (BUN), creatinine (Cre), inorganic phosphorus (Pi), and calcium (Ca) in adenine-fed and control rats. (**A**,**B**) Mesenchymal stem cells (MSCs) transplantation significantly reduced serum BUN ($P < 0.05$) and Cr ($P < 0.05$) levels on day 42. (**C**,**D**,**G**) MSCs significantly reduced serum Pi ($P < 0.05$), FGF23 ($P < 0.05$), and intact parathyroid hormone (PTH) ($P < 0.05$) on day 56 as compared to those in the control group. (**D**,**F**). Serum levels of Ca and 1–25$(OH)_2D_3$ on day 56 did not significantly differ between the MSC and control groups. Data are expressed as the mean ± SEM.

adenine-induced kidney damage is not directly because of the differentiation of MSCs, but rather is mediated by the metabolic function of MSCs.

Ca and Pi levels in the thoracic aorta significantly correlate with serum Ca and Pi levels. We next analyzed the correlation between Ca and Pi levels in the thoracic aorta and serum Ca and Pi levels at the time of sacrifice in Experiment 1. Pi and Ca levels in the aorta significantly correlated with the Ca × Pi product and serum Pi levels at the time of sacrifice (Fig. 8). This suggested that the inhibitory effect of MSCs transplantation on vascular calcification depends on serum Pi levels.

Discussion

In this study, we analyzed the effects of autologous MSCs transplantation on the progression of kidney damage and vascular calcification in an adenine-induced CKD model. We found that MSCs transplantation reduced adenine-induced kidney injury and the progression of vascular calcification, suggesting that this could represent a promising treatment option for patients with CKD.

Cardiovascular disease (CVD) is a major cause of morbidity and mortality for CKD patients waiting for kidney transplantation, and it is the most common cause of death in transplant recipients[29]. Many nephrologists pay strive to prevent CVD in CKD patients to improve long-term outcomes[30]. Therefore, new modalities to prevent the progression of vascular calcification are urgently needed. In this study, we demonstrated for the first time that MSCs transplantation reduces vascular calcification using an adenine-induced CKD model. If this therapy were to be clinically applied, it might contribute to improved prognosis for not only CKD patients, but also kidney transplant recipients.

Vascular calcification in CKD is thought to be due to the induction of osteoblastic phenotypic changes, which result from several factors including not only hyperphosphatemia, but also uremic toxins, oxidative stress, and haemodynamic state[31]. Inhibition of these factors has been shown to effectively prevent vascular calcification[32–36]. In adenine-induced CKD rats, vascular calcification generally correlates with the serum Ca × Pi product[26,37] and

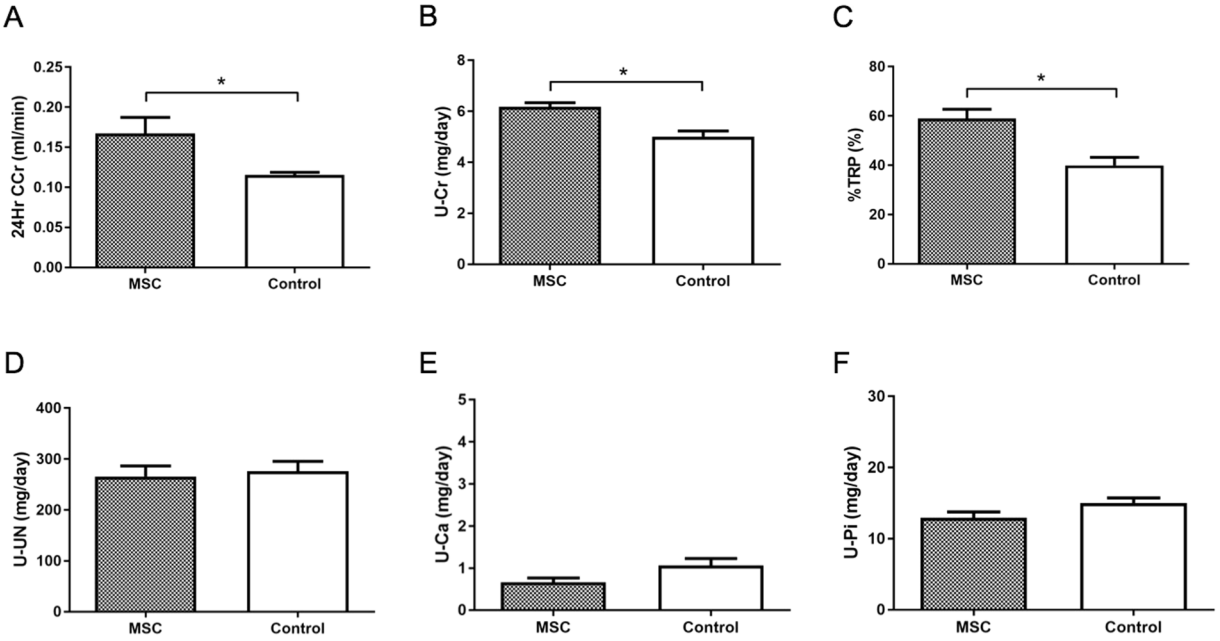

Figure 4. Urinary parameters in adenine-fed rats. (**A**–**C**) Mesenchymal stem cells (MSCs) transplantation significantly elevated 24-h creatinine clearance (24-h CCr) ($P < 0.05$), urine creatinine (Cr) ($P < 0.005$), and the tubular reabsorption of phosphate (%TRP) ($P < 0.005$) on day 56 as compared to those in the control group. (**D**–**F**) Urinary levels of blood urea nitrogen (BUN), calcium (Ca), and inorganic phosphorus (Pi) on day 56 did not significantly differ between the MSC and control groups. Data are expressed as the mean ± SEM.

can be decreased by administering phosphorus-binding agents[32–34]. In our study, Pi and Ca levels in the aorta significantly correlated with the Ca × Pi product, as well as with serum Pi levels, as previously reported[26,37]. Serum Pi levels in the MSC group were lower than those in the control group. Therefore, these results suggest that the suppression of kidney damage and improvement of kidney function lead to a decline in the serum Pi levels, and that the Ca × Pi product depends on residual kidney function, resulting in amelioration of vascular calcification.

A recent study showed that Gli1+ MSC-like cells are critical adventitial progenitors for vascular remodelling[22]. Thus, we analyzed whether injected MSCs migrate into the media using Luc+ MSCs. The results showed that injected MSCs did not migrate into the media, suggesting that MSCs transplantation does not negatively affect vascular calcification during CKD.

MSCs additionally inhibit oxidative stress[14,29], which is reportedly associated with vascular calcification[38,39]. We did not examine the effect of MSCs transplantation on the oxidative stress of vessels or the hemodynamic state. Moreover, there is a possibility that soluble factors or microvesicles derived from MSCs directly attenuate pre-existing vascular calcification. However, we did not generate data regarding the effect of MSCs on pre-existing vascular calcification. Therefore, further studies are needed to determine the exact mechanism through which MSCs transplantation affects vascular calcification.

Studies using various renal injury models have demonstrated the ability of MSCs to repair kidney damage and attenuate renal fibrosis through modulation of the immune system[40], the reduction in oxidative stress[14,41], the secretion of soluble factors such as hepatocyte growth factor (HGF) and vascular endothelial growth factor (VEGF)[17–19,21], and microvesicles[20,41]. Our study showed that injected Luc+ MSCs do not migrate into the damaged kidneys, suggesting that the mechanism for kidney repair in this study involves soluble factors (e.g., VEGF) as previously reported[21] or microvesicles derived from the MSCs. In contrast, the serum levels of Cr at the time of sacrifice were not significantly different between MSCs-treated and control rats in our study. A recent study showed that adenine induces interstitial nephritis and polyuria, resulting in dehydration[2]; thus, to evaluate the degree of dehydration, we analyzed hematocrit (Ht) levels in rats on day 42. These were higher in the MSCs-treated group than in the control group (Supplementary Fig. 2, $P < 0.005$), suggesting that the former group was more affected by dehydration. In contrast, urinary parameters indicated that 24-h CCr and urinary Cr excretion were significantly higher in the MSCs-treated group than in the control group (Fig. 4A,B). From these results, we suggest that dehydration induced an elevation in serum Cr levels in the MSCs-treated group, resulting in the discrepancy between pathology and serum Cr levels in this study.

In conclusion, to our knowledge, we demonstrated for the first time that MSCs transplantation has beneficial effects on vascular calcification in adenine-induced CKD rats. The renoprotective effect of MSCs is regarded as one of the mechanisms through which vascular calcification is suppressed. Our findings suggest that MSCs transplantation has potential as a new therapeutic strategy for the treatment of vascular calcification in patients with CKD.

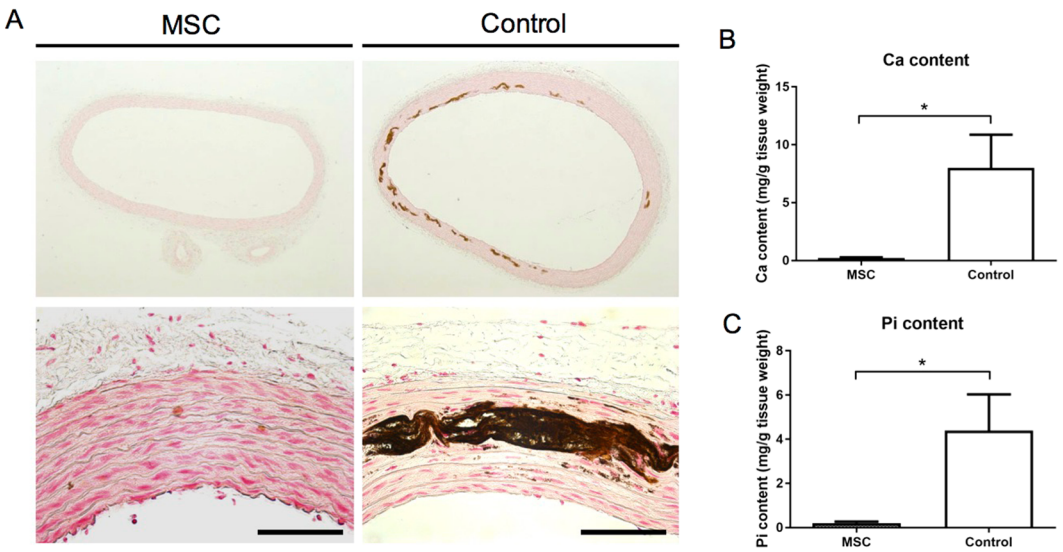

D

Kossa positive score

	MSC					Control				
Number of	<20%	20-40%	40-60%	60-80%	80%<	<20%	20-40%	40-60%	60-80%	80%<
Rats	7	0	0	0	0	4	0	1	0	4

*P<0.05

Figure 5. Effect of mesenchymal stem cells (MSCs) transplantation on calcification of the aortic media. (**A**) Von Kossa staining of the thoracic aorta media revealed that MSCs transplantation suppressed vascular calcification as compared to that in the control group. (**B**,**C**) MSCs transplantation reduced calcium ($P < 0.0005$) and phosphorus ($P < 0.01$) contents in the thoracic aorta as compared to those in the control group. (**D**) Calcification scores in the MSC group were significantly lower than those in the control group ($P < 0.05$). Data are expressed as the mean ± SEM. Black scale bars: 100 μm.

Materials and Methods

Ethics statement. All experimental procedures were approved by the Animal Committee of the Jikei University School of Medicine and conducted according to the Fundamental Guidelines for Proper Conduct of Animal Experiments and Related Activities in Academic Research Institutions issued by the Japanese Ministry of Education, Culture, Sports, Science and Technology. All surgeries were performed under isoflurane anaesthesia and all efforts were made to minimize suffering.

Experimental protocols. *Experiment 1.* Adult male SD rats (9 weeks of age) were purchased from Japan SLC (Hamamatsu, Japan) and were fed a standard CE-2 diet (Nihon CLEA, Tokyo, Japan). They were kept in cages in pairs and allowed free access to food and water. Adipose tissue was dissected from around the groin area and the femur of rats (day 1). After 4 weeks (at 13 weeks of age), the rats were divided into two groups: an adenine control group (n = 9) and an MSC group (n = 7), and were fed a CE-2 diet containing 0.75% adenine (Wako, Osaka, Japan) for 4 weeks. Following adenine feeding, rats were injected with 5×10^5 MSCs resuspended in 1 ml of PBS or vehicle control (1 ml of PBS) via the tail vein every week (days 28, 35, 42, 49, and 56). Blood was sampled from the tail vein every two weeks (days 28, 42, and 56). The rats were placed in metabolic cages for 24-h urine collection on day 56. After 4 weeks of the adenine diet (at 17 weeks of age), adenine-treated rats were returned to a normal diet. After 2 days of normal diet (day 58), all animals were sacrificed by abdominal aortic puncture under isoflurane anaesthesia. The experimental design is summarized in Supplementary Fig. S3.

Experiment 2. Adult male Lewis rats (10 weeks old) were purchased from Japan SLC (Hamamatsu, Japan) and were fed a standard CE-2 diet (Nihon CLEA). After 1 week (at 11 weeks of age), the rats were divided into two groups: an adenine control group (n = 4) and a Luc-MSC group (n = 4), and were fed a CE-2 diet containing 0.75% adenine (Wako, Osaka, Japan) for 4 weeks. Following adenine feeding, the rats were injected with 5×10^5 luciferase-expressing (Luc+) MSCs resuspended in 1 ml of PBS or vehicle control (1 ml of PBS) via the tail vein every week (days 7, 14, 21, 28, and 35). After 4 weeks of the adenine diet (at 15 weeks of age), adenine-treated rats were returned to a normal diet. After 1 week of the normal diet (day 42), all animals were sacrificed by abdominal aortic puncture under isoflurane anesthesia. The experimental design is summarized in Supplementary Fig. S4.

MSCs culture. MSCs were isolated as previously described[27,42]. Briefly, adipose tissues were minced using scissors and washed with phosphate-buffered saline (PBS) (Thermo Fisher Scientific, Waltham, MA, USA) and

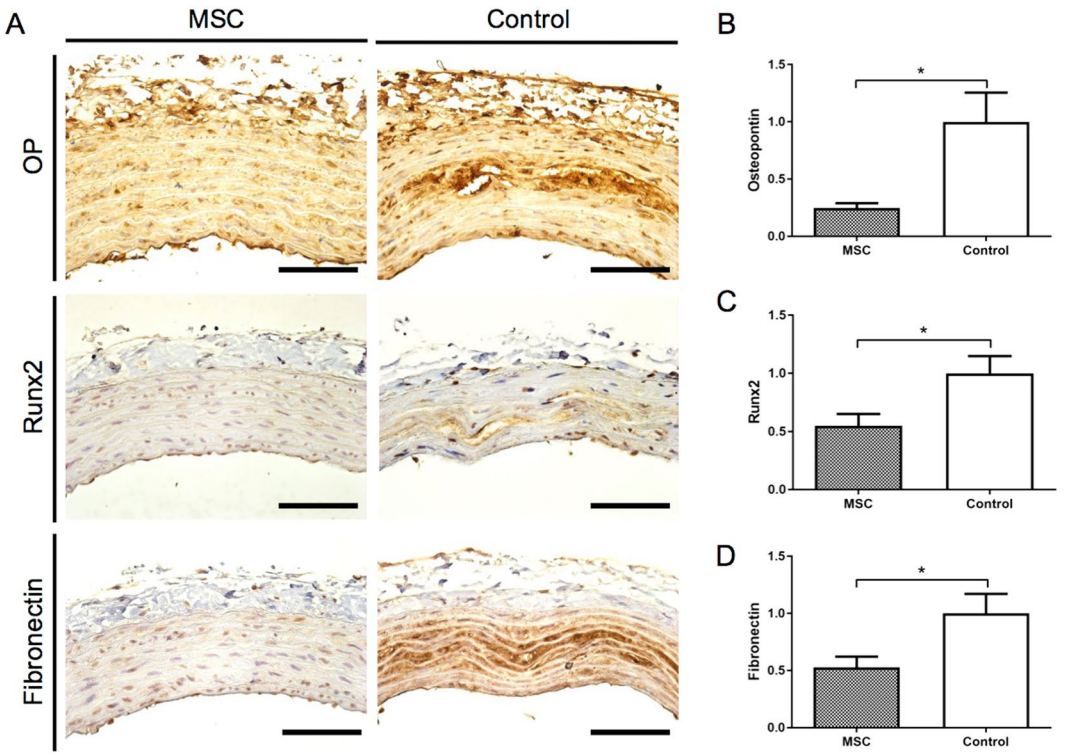

Figure 6. Expression of osteopontin (OP), Runx2, and fibronectin in the thoracic aorta. (**A**) Expression of OP, Runx2, and fibronectin in the thoracic aorta was detected by immunohistochemistry. (**B**–**D**) OP ($P < 0.05$), Runx2 ($P < 0.05$), and fibronectin ($P < 0.05$) mRNA expression were significantly suppressed in the MSC group as compared to the control group. Data are expressed as the mean ± SEM. Black scale bars: 100 μm.

were then enzymatically dissociated with 1 ml of 0.1% collagenase (type I) (Wako, Osaka, Japan) in PBS for 1 h at 37 °C. The dissociated tissue was incubated in α-minimum essential medium (αMEM) (Thermo Fisher Scientific) supplemented with foetal bovine serum (FBS) (Thermo Fisher Scientific), and centrifuged. The cell pellet was resuspended in PBS. After centrifugation, adipose cells including MSCs were obtained. Luc+ MSCs were obtained from adipose tissues of luciferase transgenic rats[6,43]. Isolated cells were cultured in αMEM supplemented with 20% embryonic stem cell-qualified FBS (Thermo Fisher Scientific).

Induction of adipogenesis, osteogenesis, and chondrogenesis. Multilineage differentiation of MSCs under adipogenic, chondrogenic, and osteogenic differentiation conditions was analyzed as previously described[27]. Briefly, MSCs were seeded in induction medium with MSC differentiation kits for adipogenic, osteogenic, or chondrogenic induction (BulletKit; Lonza, Walkersville, MD). MSCs were maintained in culture according to the manufacturer's protocols.

Flow cytometry. Cells were harvested from culture by treatment with 0.05% trypsin-EDTA (Sigma-Aldrich, St Louis, MO) for 3 min at 37 °C, and approximately 1×10^6 cells were added to tubes and centrifuged at $400 \times g$ for 5 min. The pellet was washed twice in ice-cold PBS containing 2% FBS and cells were resuspended at 1×10^5 cells/antibody test. The expression of specific MSCs markers was evaluated by flow cytometry (MACSQuant; Miltenyi Biotec, Gladbach, Germany) using antibodies against CD29 (BD, New Jersey, USA), CD31 (Thermo Fisher Scientific, Waltham, MA, USA), CD45 (R&D systems, MN, USA), and CD90 (BD Biosciences Pharmingen, Tokyo, Japan).

Bioluminescence imaging. Luc+ MSCs (5×10^5 per rat) from luciferase-transgenic rats were injected into the Luc-MSC group rats via the tail vein every week. Rats were anaesthetized with 2.0% (vol/vol) isoflurane, injected intravenously with 1 ml D-luciferin (33 mg/ml in PBS; Summit Pharmaceuticals International Corp., Tokyo, Japan) and imaged for 10 min on days 0 (1 h post Luc+ MSCs injection), day 1 (24 h post Luc+ MSCs injection), and day 2 (48 h post Luc+ MSCs injection) using the Xenogen IVIS 200 system (Xenogen, Alameda, CA). The experimental design is summarized in Supplementary Fig. S4.

Blood and urinary biochemistry. Blood and urine samples were analyzed as previously described[26]. Briefly, serum Pi, Ca, BUN, and Cr levels were measured using an automated analyzer (FDC-3500; Fuji Film, Tokyo, Japan). Urinary Cr, Pi, and Ca levels were analyzed according to the manufacturer's instructions (SRL, Tokyo, Japan). Serum concentrations of PTH and FGF23 were determined by enzyme-linked immunosorbent assay (ELISA) with a rat intact PTH ELISA kit (Immutopics, Inc., San Clemente, CA) and FGF-23 ELISA kit

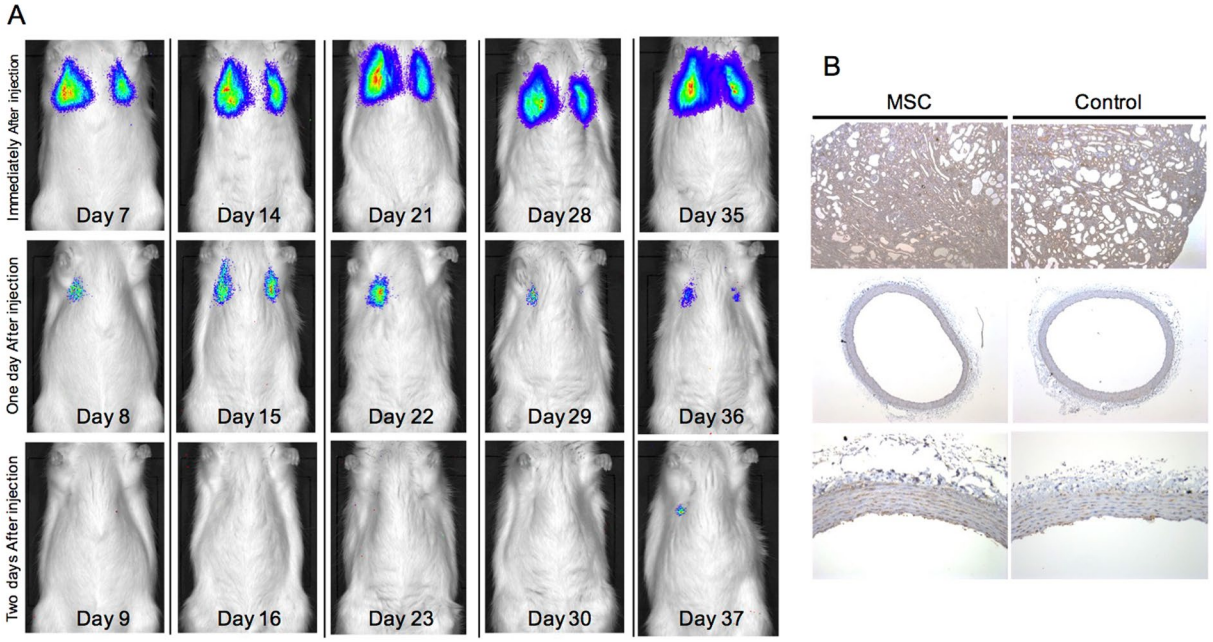

Figure 7. *In vivo* imaging of luciferase positive (Luc+) mesenchymal stem cells. (**A**) Luminescence was observed bilaterally in the lungs, but not in the kidneys. The signal disappeared on the third day. (**B**) Expression of luciferase was not detected by immunohistochemistry.

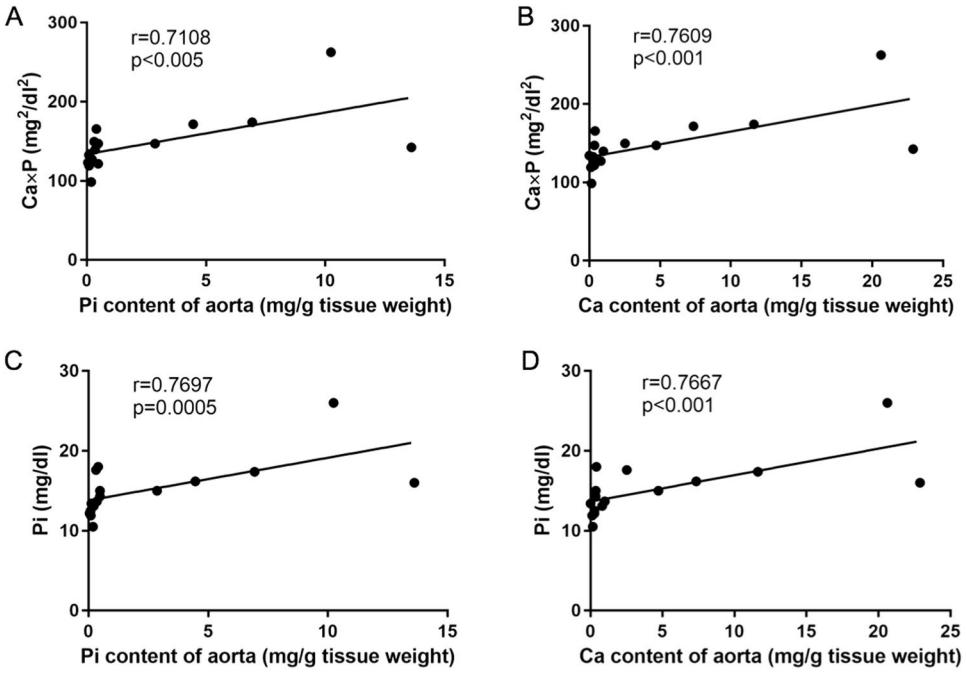

Figure 8. Correlation between the inorganic phosphorous (Pi) or calcium (Ca) content of the thoracic aorta and serum Pi or the Ca × Pi product at time of sacrifice. (**A**,**B**) Linear correlation between the Pi or Ca content of the thoracic aorta and the Ca × Pi product at the time of sacrifice ($P < 0.005$, $P < 0.001$, respectively). (**C**,**D**) Linear correlation between the Pi or Ca content of the thoracic aorta and serum Pi ($P < 0.0005$, $P < 0.001$, respectively).

(Kainos Laboratories Inc., Tokyo, Japan). The serum levels of 1-α25-dihydroxyvitamin D3 (1–25$(OH)_2D_3$) were measured using a radioimmunoassay according to the manufacturer's instructions (SRL).

Histopathological examinations. For histopathological examination, all resected tissues were fixed with 10% buffered formalin, and 5-μm-thick sections were stained with haematoxylin–eosin. Adipocytes differentiated

from MSCs were stained with Sudan III. Osteoblasts differentiated from MSCs were stained by the von Kossa method. Chondrocytes differentiated from MSCs were stained with Safranin O, Fast green, and Toluidine blue using a Cartilage Staining Kit (Takara Bio, Tokyo, Japan)[27,42]. Kidney sections were stained using the Masson trichrome method. The dimensions of tubular lumen dilatation and the degree of interstitial fibrosis, as well as the glomerular numbers were quantified from 10 high-power fields of the cortical area per section using MetaValue software (Molecular Devices, Sunnyvale, CA) and a BIOREVO BZ-9000 microscope (Keyence, Osaka, Japan) as previously described[7]. The kidney sections were also examined immunohistochemically for the expression of ED-1 (ab31630; Abcam, Cambridge, UK), AQP 1 (sc-20810; Santa Cruz Biotechnology, Inc, Dallas, TX), and luciferase (PM016; MBL, Nagoya, Japan). Areas of positive staining were quantified using MetaValue. Aorta sections were stained using the von Kossa method and scored semi-quantitatively for Kossa-positive areas using a previously described scoring system[26] with a slight modification. Aortic tissue was also examined for the expression of osteopontin (LB4225; LSL, Tokyo, Japan), Runx2 (sc-8566; Santa Cruz Biotechnology, Inc), fibronectin (sc-9068; Santa Cruz Biotechnology, Inc), and luciferase (MBL) using monoclonal antibodies.

Ca and Pi contents in thoracic aorta. The levels of Ca and Pi in the aorta were determined as described previously[26]. Briefly, thoracic aortas were weighed shortly after removal and were subsequently extracted with 150 mM HCl overnight at room temperature to dissolve any minerals. The levels of Ca and Pi in the solution were analysed according to the manufacturer's instructions (Wako, Osaka, Japan). The levels of Ca and Pi in the aorta were calculated as the weight of calcium or phosphorus per wet tissue weight of aorta.

RNA isolation and real-time reverse transcriptase polymerase chain reaction (qRT-PCR). RNA was extracted from tissues using TRIzol Reagent (Thermo Fisher Scientific) according to the manufacturer's instructions. Genomic DNA was removed using DNase I (Takara Bio, Otsu, Japan) and cDNA was synthesized from the total RNA using the Superscript RT-PCR system. Osteopontin, Runx2, and fibronectin mRNA levels were semi-quantified by qRT-PCR using an ABI7000 (Thermo Fisher Scientific) with RT2 SYBR Green Master Mix (Qiagen, Hilden, Germany) and a Rat osteogenesis PCR Array (Qiagen) according to the manufacturer's instructions.

Statistical analysis. Data are presented as the mean ± SEM. Statistical analyses were carried out using GraphPad Prism 5 (GraphPad Software, San Diego, CA). The significance of differences between two mean values was determined using unpaired *t*-tests. The Pearson correlation coefficient was used to evaluate the correlation between the Ca and P contents of the aorta and serum Ca × P products. Statistical significance was defined as $P < 0.05$.

References

1. Lozano, R. *et al*. Global and regional mortality from 235 causes of death for 20 age groups in 1990 and 2010: a systematic analysis for the Global Burden of Disease Study. *Lancet* **380**, 2095–2028 (2012).
2. Yokote, S. *et al*. The effect of metanephros transplantation on blood pressure in anephric rats with induced acute hypotension. *Nephrol. Dial. Transplant.* **27**, 3449–3455 (2012).
3. Liyanage, T. *et al*. Worldwide access to treatment for end-stage kidney disease: a systematic review. *Lancet* **385**, 1975–1982 (2015).
4. Yokoo, T. *et al*. Human mesenchymal stem cells in rodent whole-embryo culture are reprogrammed to contribute to kidney tissues. *Proc. Natl. Acad. Sci. USA* **102**, 3296–3300 (2005).
5. Yokoo, T. *et al*. Xenobiotic kidney organogenesis from human mesenchymal stem cells using a growing rodent embryo. *J. Am. Soc. Nephrol.* **17**, 1026–1034 (2006).
6. Matsumoto, K. *et al*. Xenotransplanted embryonic kidney provides a niche for endogenous mesenchymal stem cell differentiation into erythropoietin-producing tissue. *Stem Cells* **30**, 1228–1235 (2012).
7. Yokote, S. *et al*. Urine excretion strategy for stem cell-generated embryonic kidneys. *Proc. Natl. Acad. Sci. USA* **112**, 12980–12985 (2015).
8. Taguchi, A. *et al*. Redefining the *in vivo* origin of metanephric nephron progenitors enables generation of complex kidney structures from pluripotent stem cells. *Cell. Stem Cell* **14**, 53–67 (2014).
9. Sharmin, S. *et al*. Human induced pluripotent stem cell-derived podocytes mature into vascularized glomeruli upon experimental transplantation. *J. Am. Soc. Nephrol.* **27**, 1778–1791 (2016).
10. Takasato, M. *et al*. Kidney organoids from human iPS cells contain multiple lineages and model human nephrogenesis. *Nature* **526**, 564–568 (2015).
11. Morizane, R. *et al*. Nephron organoids derived from human pluripotent stem cells model kidney development and injury. *Nat. Biotechnol.* **33**, 1193–1200 (2015).
12. Morigi, M. & Benigni, A. Mesenchymal stem cells and kidney repair. *Nephrol. Dial. Transplant.* **28**, 788–793 (2013).
13. Gu, W., Hong, X., Potter, C., Qu, A. & Xu, Q. Mesenchymal stem cells and vascular regeneration. *Microcirculation* **24**, https://doi.org/10.1111/micc.12324 (2017).
14. Ashour, R. H. *et al*. Comparative study of allogenic and xenogeneic mesenchymal stem cells on cisplatin-induced acute kidney injury in Sprague-Dawley rats. *Stem Cell Res. Ther.* **7**, 126, https://doi.org/10.1186/s13287-016-0386-0 (2016).
15. Anan, H. H., Zidan, R. A., Shaheen, M. A. & Abd-El Fattah, E. A. Therapeutic efficacy of bone marrow derived mesenchymal stromal cells versus losartan on adriamycin-induced renal cortical injury in adult albino rats. *Cytotherapy* **18**, 970–984 (2016).
16. Monteiro Carvalho Mori da Cunha, M. G. *et al*. Amniotic fluid derived stem cells with a renal progenitor phenotype inhibit interstitial fibrosis in renal ischemia and reperfusion injury in rats. *PLoS One* **10**, e0136145 (2015).
17. Jiang, M. H. *et al*. Nestin(+) kidney resident mesenchymal stem cells for the treatment of acute kidney ischemia injury. *Biomaterials* **50**, 56–66 (2015).
18. Villanueva, S. *et al*. Mesenchymal stem cell injection ameliorates chronic renal failure in a rat model. *Clin Sci. (Lond).* **121**, 489–499 (2011).
19. Villanueva, S. *et al*. Human mesenchymal stem cells derived from adipose tissue reduce functional and tissue damage in a rat model of chronic renal failure. *Clin Sci. (Lond).* **125**, 199–210 (2013).
20. Merino-González, C. *et al*. Mesenchymal stem cell-derived extracellular vesicles promote angiogenesis: potential clinical application. *Front. Physiol.* **7**, 24 https://doi.org/10.3389/fphys.2016.00024. eCollection 2016 (2016).
21. Jia, X. *et al*. Bone marrow mesenchymal stromal cells ameliorate angiogenesis and renal damage via promoting PI3k-Akt signaling pathway activation *in vivo*. *Cytotherapy* **18**, 838–845 (2016).

22. Kramann, R. *et al.* Adventitial MSC-like cells are progenitors of vascular smooth muscle cells and drive vascular calcification in chronic kidney disease. *Cell Stem Cell.* **19**, 628–642 (2016).
23. Liao, J. *et al.* Transfer of bone-marrow-derived mesenchymal stem cells influences vascular remodeling and calcification after balloon injury in hyperlipidemic rats. *J. Biomed. Biotechnol.* **2012**, 165296, https://doi.org/10.1155/2012/165296 (2012).
24. Kramann, R. *et al.* Exposure to uremic serum induces a procalcific phenotype in human mesenchymal stem cells. *Arterioscler. Thromb. Vasc Biol.* **31**, e45–54 (2011).
25. Kramann, R. *et al.* Osteogenesis of heterotopically transplanted mesenchymal stromal cells in rat models of chronic kidney disease. *J. Bone Miner. Res.* **28**, 2523–2534 (2013).
26. Yokote, S. *et al.* Metanephros transplantation inhibits the progression of vascular calcification in rats with adenine-induced renal failure. *Nephron Exp. Nephrol.* **120**, e32–40 (2012).
27. Yamada, A. *et al.* Comparison of multipotency and molecular profile of MSCs between CKD and healthy rats. *Hum. Cell* **27**, 59–67 (2014).
28. Klinkhammer, B. M. *et al.* Mesenchymal stem cells from rats with chronic kidney disease exhibit premature senescence and loss of regenerative potential. *PLoS One* **9**, e92115 (2014).
29. Collins, A. US renal data system 2012 annual report. *Am. J. Kidney Dis.* **6**, A7 (2013).
30. Hart, A. *et al.* Cardiovascular risk assessment in kidney transplantation. *Kidney Int.* **87**, 527–534 (2015).
31. Tatsumoto, N. *et al.* Spironolactone ameliorates arterial medial calcification in uremic rats: the role of mineralocorticoid receptor signaling in vascular calcification. *Am. J. Physiol. Renal Physiol.* **309**, F967–979 (2015).
32. Yamada, S. *et al.* Phosphate binders prevent phosphate-induced cellular senescence of vascular smooth muscle cells and vascular calcification in a modified, adenine-based uremic rat model. *Calcif. Tissue Int.* **96**, 347–358 (2015).
33. Katsumata, K. *et al.* Sevelamer hydrochloride prevents ectopic calcification and renal osteodystrophy in chronic renal failure rats. *Kidney Int.* **64**, 441–450 (2003).
34. Neven, E. *et al.* Adequate phosphate binding with lanthanum carbonate attenuates arterial calcification in chronic renal failure rats. *Nephrol. Dial. Transplant.* **24**, 1790–1799 (2009).
35. Adijang, A., Higuchi, Y., Nishijima, F., Shimizu, H. & Niwa, T. Indoxyl sulfate, a uremic toxin, promotes cell senescence in aorta of hypertensive rats. *Biochem. Biophys. Res. Commun.* **399**, 637–641 (2010).
36. Yamada, S. *et al.* The antioxidant tempol ameliorates arterial medial calcification in uremic rats: important role of oxidative stress in the pathogenesis of vascular calcification in chronic kidney disease. *J. Bone Miner. Res.* **27**, 474–485 (2012).
37. Terai, K. *et al.* Vascular calcification and secondary hyperparathyroidism of severe chronic kidney disease and its relation to serum phosphate and calcium levels. *Br. J. Pharmacol.* **156**, 1267–1278 (2009).
38. Byon, C. H. *et al.* Oxidative stress induces vascular calcification through modulation of the osteogenic transcription factor Runx2 by AKT signaling. *J. Biol. Chem.* **283**, 15319–15327 (2008).
39. Farrar, E. J., Huntley, G. D. & Butcher, J. Endothelial-derived oxidative stress drives myofibroblastic activation and calcification of the aortic valve. *PLoS One* **10**, e0123257 (2015).
40. Peired, A. J., Sisti, A. & Romagnani, P. Mesenchymal stem cell-based therapy for kidney disease: a review of clinical evidence. *Stem Cells Int.* **2016**, 4798639 (2016).
41. Zhou, Y. *et al.* Exosomes released by human umbilical cord mesenchymal stem cells protect against cisplatin-induced renal oxidative stress and apoptosis *in vivo* and *in vitro*. *Stem Cell Res. Ther.* **4**, 34 (2013).
42. Yamanaka, S. *et al.* Adipose tissue-derived mesenchymal stem cells in long-term dialysis patients display downregulation of PCAF expression and poor angiogenesis activation. *PLoS One* **9**, e102311 (2014).
43. Hakamata, Y., Murakami, T. & Kobayashi, E. "Firefly rats" as an organ/cellular source for long-term *in vivo* bioluminescent imaging. *Transplantation* **81**, 1179–1184 (2006).

Acknowledgements

This work was supported by KAKENHI Grant Number JP16K19499.

Author Contributions

S.Y. designed the experiments. S.Y., Y.K., and A.Y. performed the experiments. S.Y. and I.O. analyzed the data. S.Y. and T.Y. wrote the paper.

Additional Information

Supplementary information accompanies this paper at https://doi.org/10.1038/s41598-017-14492-9.

Competing Interests: The authors declare that they have no competing interests.

Publisher's note: Springer Nature remains neutral with regard to jurisdictional claims in published maps and institutional affiliations.